JOURNAL OF BACTERIOLOGY, Nov. 2010, p. 5682–5687 Vol. 192, No. 21
0021-9193/10/$12.00 doi:10.1128/JB.00674-10

Regulation of a Phage Endolysin by Disulfide Caging▽

Gabriel F. Kuty, Min Xu,† Douglas K. Struck, Elizabeth J. Summer, and Ry Young*

Department of Biochemistry and Biophysics, Texas A&M University, 2128 TAMU, College Station, Texas 77843-2128

Received 11 June 2010/Accepted 26 August 2010

In contrast to canonical phage endolysins, which require holin-mediated disruption of the membrane to gain access to attack the cell wall, signal anchor release (SAR) endolysins are secreted by the host *sec* system, where they accumulate in an inactive form tethered to the membrane by their N-terminal SAR domains. SAR endolysins become activated by various mechanisms upon release from the membrane. In its inactive form, the prototype SAR endolysin, Lyz_{P1}, of coliphage P1, has an active-site Cys covalently blocked by a disulfide bond; activation involves a disulfide bond isomerization driven by a thiol in the newly released SAR domain, unblocking the active-site Cys. Here, we report that Lyz_{103}, the endolysin of *Erwinia* phage ERA103, is also a SAR endolysin. Although Lyz_{103} does not have a catalytic Cys, genetic evidence suggests that it also is activated by a thiol-disulfide isomerization triggered by a thiol in the SAR domain. In this case, the inhibitory disulfide in nascent Lyz_{103} is formed between cysteine residues flanking a catalytic glutamate, caging the active site. Thus, Lyz_{P1} and Lyz_{103} define subclasses of SAR endolysins that differ in the nature of their inhibitory disulfide, and Lyz_{103} is the first enzyme found to be regulated by disulfide bond caging of its active site.

In infections by double-stranded DNA phages, host lysis requires degradation of the peptidoglycan by a phage-encoded endolysin (17). By far the most intensively studied endolysin is the T4 lysozyme E (EC 3.2.1.17), which attacks the glycosidic bonds between GlcNAc and MurNAc in the murein (1). During the latent period, canonical endolysins are produced as fully active enzymes sequestered in the cytoplasm, thereby preventing premature lysis. Another phage protein, the holin, terminates the infection cycle by suddenly forming extremely large, nonspecific holes in the membrane that allow the endolysin to escape and attack the murein layer. Recently, studies of the lysis system of bacteriophage P1 have revealed that phage-encoded endolysins are not always dependent upon holins for export (19, 20). Although it is an ortholog of T4 E, the P1 lysozyme, Lyz_{P1}, is translocated across the cytoplasmic membrane by the host *sec* system by virtue of an N-terminal transmembrane domain (TMD) that is absent in E (Fig. 1A). Since this transmembrane domain is not removed by signal peptidase, nascent Lyz_{P1} remains tethered to the membrane with its catalytic residues already present in the periplasm. The Lyz_{P1} TMD exits the membrane and becomes part of the soluble, periplasmic form of the protein, either at a low spontaneous rate or, more efficiently, when the holin triggers to depolarize the membrane (11). Because of the unique ability to direct *sec*-mediated export and membrane insertion and to support release into the periplasm from the bilayer, the TMD of Lyz_{P1} was designated a signal anchor release (SAR) domain. More recently, other SAR endolysins have been identified and characterized (15, 16). In fact, bioinformatic analysis suggests that most members of the T4 lysozyme family, recognizable by the Glu-8aa-(Asp/Cys)-5aa-Thr catalytic triad (Fig. 1A), are SAR endolysins (43 of 58 entries in the GenBank protein database) (16).

Since the lyz_{P1} gene is expressed well before progeny P1 phage have been assembled, there must be a mechanism to ensure that the membrane-tethered form of the protein is kept enzymatically inactive so that premature lysis is avoided. A key to the regulation of Lyz_{P1} is the fact that the P1 enzyme has a catalytic cysteine residue, Cys_{51} (Fig. 1A), in the central position of the catalytic triad, in contrast to E and most of its orthologs, which have an Asp residue in this position (20). Genetic, biochemical, and structural analysis of Lyz_{P1} demonstrated that the membrane-tethered form is inactive for two reasons: first, the entire catalytic domain is misfolded, so the active-site cleft is completely missing, and second, the catalytic Cys_{51} is covalently occupied in a disulfide bond with another Cys at position 44. This led to a model for activation in which a thiol (Cys_{13}) present in the SAR domain becomes unmasked upon membrane release and triggers a disulfide bond isomerization, liberating the thiol of the catalytic Cys_{51}. This model was confirmed by crystal structures showing the alternative disulfide linkages in the inactive and active forms of Lyz_{P1} (19).

Lyz_{P1} became the prototype of a class of SAR endolysins recognizable by the Asp→Cys substitution in the catalytic triad and the presence of activating Cys in the N-terminal SAR domain. However, most SAR endolysins belong to a second major class, represented by R_{21}, the endolysin of the lambdoid phage 21 (20). These enzymes have the canonical Glu-8aa-Asp-5aa-Thr catalytic triad and no Cys residue in the SAR domain. Instead, genetic and structural analysis revealed that in the inactive form, the catalytic domain has nearly the correct fold, except for a displacement of the active-site Glu, but is subject to steric hindrance by the proximity of the bilayer in which the SAR domain is embedded. In the soluble, active form, the SAR domain of R_{21} has refolded into the main body of the enzyme, providing a floor to the active site and reposi-

* Corresponding author. Mailing address: 2128 TAMU, Department of Biochemistry and Biophysics, Texas A&M University, College Station, TX 77843-2128. Phone: (979) 845-2087. Fax: (979) 862-4718. E-mail: ryland@tamu.edu.

† Present address: 3270 Sawtelle Blvd., Apt. 101, Los Angeles, CA 90066.

▽ Published ahead of print on 10 September 2010.

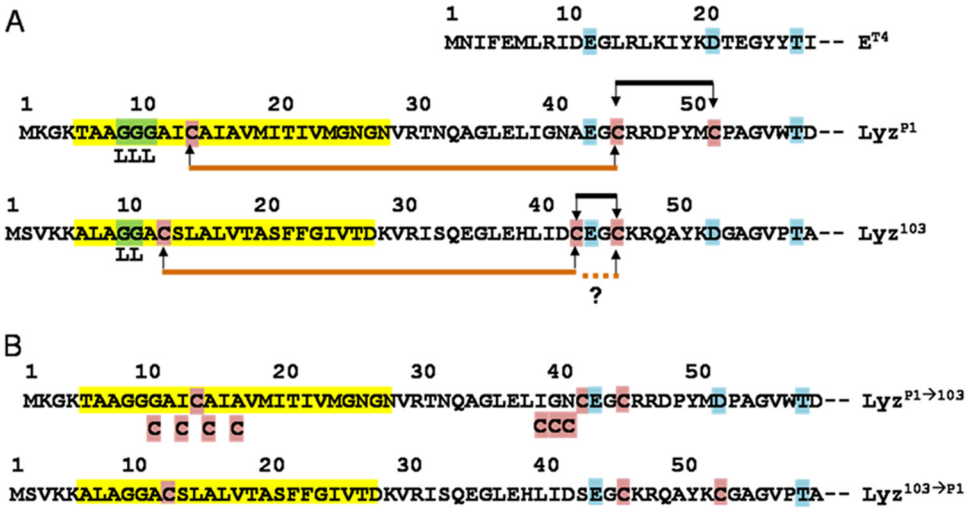

FIG. 1. Sequence alignments. (A) Alignment of T4E, Lyz_{P1}, and Lyz_{103}. Catalytic residues are highlighted in blue, Cys residues in pink, and SAR domains in yellow. Locations of Leu substitutions are indicated below the corresponding Gly residue (green). Inactivating/caging disulfides for Lyz_{P1} and Lyz_{103}, respectively, are shown as arrows connected with a black line above the participating Cys residues. Disulfides resulting from isomerization are shown below the participating Cys residues as arrows connected with a brown line. (B) Alignments of $Lyz_{P1\rightarrow103}$ and $Lyz_{103\rightarrow P1}$ conversion mutants. Catalytic residues are highlighted in blue, Cys residues in pink, and SAR domains in yellow. Locations of Cys substitutions are indicated below the corresponding residue.

tioning the catalytic glutamate to its proper place (16). Thus, the R_{21} regulatory scheme is markedly different from that of Lyz_{P1}, where the released SAR domain provides only the free thiol for the disulfide bond rearrangement and makes few contacts with the enzyme itself.

Here, we examine the regulation of the endolysin Lyz_{103} of the *Erwinia amylovora* phage ERA103 (GenBank accession no. EF160123), which seems to have characteristics of both of these major classes: it has a Cys residue in an N-terminal hydrophobic sequence but retains the canonical Asp residue in the catalytic triad. The results are discussed in terms of a model for SAR-dependent disulfide bond isomerization distinct from that of Lyz_{P1} and its homologs but which nevertheless confers a covalent constraint on premature activation of the muralytic activity.

MATERIALS AND METHODS

Bacterial strains and growth conditions. The *Escherichia coli* strains XL1-Blue and MC4100 and the MG1655 Δ*fhuA lacI*^{q} *lacY* mutant strain have been described previously (13, 16). Standard conditions for the growth of cultures and the monitoring of lysis kinetics have also been described previously (3, 13). All bacterial cultures were grown in standard LB medium, supplemented with 100 μg/ml ampicillin when appropriate. When indicated, isopropyl-β-D-thiogalactopyranoside (IPTG), dinitrophenol (DNP), and dithiothreitol (DTT) were added to achieve final concentrations of 1 mM, 10 mM, and 1 mM, respectively.

DNA procedures and plasmid construction. Procedures for the isolation of plasmid DNA, DNA amplification by PCR, PCR product purification, DNA transformation, site-directed mutagenesis, and DNA sequencing have been previously described (5, 12, 14). The construction of the plasmid $pLyz_{P1}$, a derivative of pJF118EH, has been described previously (4, 20). The plasmid $pLyz_{103}$ was constructed by amplifying and inserting lyz_{103} between the EcoRI and HindIII restriction sites of pJF118EH. Similarly, the construct $pETLyz_{103}$ was constructed by amplifying lyz_{103} and inserting it between XbaI and BamHI of pET11a (Novagen). For overexpression purposes, the inactive allele $lyz_{103}(D52N)$ was used. Derivative alleles of lyz_{103} and lyz_{P1} were made using site-directed mutagenesis. For detection and purification purposes, the lyz_{103} allele was modified to encode an oligo-histidine tag ($Gly_2His_6Gly_2$) appended to Met_{178} by site-directed mutagenesis. All purified proteins cited in this work refer to the oligo-histidine-tagged versions.

SDS-PAGE and Western blotting. SDS-PAGE, Western blotting, and immunodetection experiments were performed as previously described (5). Antiserum against Lyz_{P1} was prepared in chickens by Aves Labs (Tigard, OR) and was used at a dilution of 1:1,000. A mouse monoclonal antibody against the oligo-histidine epitope tag was purchased from Amersham and was used at a dilution of 1:3,000. Horseradish peroxidase-conjugated secondary antibodies against chicken IgY were purchased from Aves Labs and were used at a 1:2,000 dilution for colorimetric detection and a 1:300,000 dilution for chemiluminescent detection. The anti-mouse IgG horseradish peroxidase-conjugated secondary antibody was supplied with the SuperSignal chemiluminescence kit (Pierce) and was used at a 1:5,000 dilution. Blots were developed using the chromogenic substrate 4-chloro-1-naphthol (Sigma) or with the West Femto SuperSignal chemiluminescence kit (Pierce). Chemiluminescent signal was detected using a Bio-Rad ChemiDoc XRS.

Subcellular fractionation. Soluble or membrane localization was determined as described previously (16, 20). Briefly, 25 ml of an induced culture was collected by centrifugation at 5,000 × *g* in a Sorvall Superspeed RC2-B centrifuge and resuspended in 2 ml of French press buffer (0.1 M sodium phosphate, 0.1 M KCl, 5 mM EDTA, 1 mM dithiothreitol, 1 mM phenylmethylsulfonyl fluoride, pH 7.0). Cells were disrupted by passage through a French pressure cell (Spectronic Instruments, Rochester, NY) at 16,000 lb/in^2. The membrane and soluble fractions were separated by centrifugation at 100,000 × *g* in a Beckman TL-100 ultracentrifuge for 60 min. Equivalent amounts of each fraction were examined by SDS-PAGE and Western blotting as described above.

Sulfhydryl modification using PEG-OPSS. To detect the presence of free cysteines in SAR endolysins, a 5-ml sample of a culture induced in logarithmic phase for 25 min was precipitated by trichloroacetic acid (TCA). The pellet was resuspended in 1 ml of PEGylation buffer (500 mM Tris [pH 7.0], 1% SDS, 1 mM EDTA), and mPEG-OPSS (Nektar Transforming Therapeutics, Huntsville, AL) (8) was added to produce a final concentration of 3 μM. The mixture was incubated for 30 min at room temperature and then precipitated by the addition of 1 ml of ice-cold acetone. The samples were held at −20°C for 10 min, after which the precipitate was collected by centrifugation at 18,000 × *g* at 4°C for 15 min. The pellets were air dried, resuspended in nonreducing SDS sample buffer, and examined by SDS-PAGE and Western blotting. All samples were run with controls that had not been exposed to PEG-OPSS.

Lyz_{103} expression and purification. Since wild-type Lyz_{103} lyses cells rapidly when overexpressed, the enzyme activity was abolished by replacing the catalytic Asp with Asn. Hence, all purified Lyz_{103} cited in this work refers to Lyz_{103}(D52N). pET $lyz_{103}(D52N)$ *cHis* was transformed into BL21(DE3) cells (Invitrogen) harboring pLysS, and fresh transformants were cultured and induced for 1 h at 30°C. Cells were collected at 4,000 rpm for 30 min at 4°C in a Sorvall RC-3B centrifuge and resuspended in Lyz_{103} buffer (20 mM Tris-HCl [pH 8], 100 mM NaCl). Protease inhibitor cocktail for His-tagged protein

(Sigma) was added as per the manufacturer's instructions, and cells were lysed by passage through a French pressure cell (Spectronic Instruments, Rochester, NY) at 20,000 lb/in^2. After unlysed cells and debris were removed, the lysate was filtered through a 0.2-μm syringe filter. The cleared lysate was then applied to Talon metal affinity resin (Clontech). Protein was eluted in elution buffer (20 mM Tris-HCl, 100 mM NaCl, 500 mM imidazole, pH 8) and was used with no further purification.

CDAP cleavage. Purified Lyz_{103}(D52N) was precipitated and resuspended in 100 μl CDAP (1-cyano-4-dimethylaminopyridinium tetrafluoroborate) buffer (4 M guanidine-HCl, 0.1 M citrate, pH 3). CDAP (Sigma), prepared fresh in CDAP buffer, was added in 1,000-fold molar excess and was incubated at room temperature for 15 min. NH_4OH (EMD Chemicals) was added to achieve a 1 M final concentration, and the mixture was incubated at room temperature for 3 h (10, 18). Total protein was precipitated by the addition of 1 ml of ice-cold ethanol and incubated overnight at −20°C. Samples were pelleted, dried, and resuspended in sample loading buffer with or without 5% β-mercaptoethanol, as indicated. Equivalent amounts were analyzed by SDS-PAGE and Western blotting.

RESULTS AND DISCUSSION

The lysozyme from bacteriophage ERA103 has an N-terminal SAR domain. We first wished to confirm that the N-terminal hydrophobic domain of Lyz_{103} is a SAR domain. Induction of *lyz*$_{103}$ resulted in lysis of *Escherichia coli*, even without a holin gene present, indicating a spontaneous release from the membrane and consequent lysis (Fig. 2A). Moreover, like Lyz_{P1}, Lyz_{103} was found in both the soluble and membrane fractions of cells (Fig. 3A). For both proteins, the membrane-associated and soluble forms migrate identically in SDS-PAGE, indicating that the latter is not derived by the proteolytic cleavage of the former. Additionally, energy poisons such as DNP accelerated the lysis of cultures expressing *lyz*$_{103}$ (Fig. 2A), indicating that the collapse of the proton motive force facilitates the membrane release and activation of Lyz_{103}, as it does for Lyz_{P1} (20). The SAR domains characterized in Lyz_{P1} and R_{21} differ from conventional TMDs in that they have a high content of weakly hydrophobic and uncharged polar residues, such as Ala, Gly, and Ser (20). In both cases, substitution of Leu residues for Gly residues (3 in Lyz_{P1} [Fig. 2, 3C] and 2 in R_{21} [16]) in the SAR domain blocked the release from the membrane and host lysis. The same molecular and cellular phenotype was observed for Lyz_{103} when Gly residues at positions 9 and 10 in the SAR domain were converted to Leu (Fig. 2C, 3D). These results are consistent with the requirement for the SAR domain to exit the membrane, liberating the thiol in the SAR domain to attack the inhibitory disulfide. Thus, Lyz_{103} is the third SAR endolysin to be characterized in terms of its physiological and topological characteristics. The predicted amino acid sequence of Lyz_{103} is identical to that of the lysozyme from bacteriophage ϕEa1h. Thus, the puzzling lethality observed when *lyz*$^{\phi Ea1h}$ was expressed in the absence of its holin (6, 7) is due to the fact that, as a SAR endolysin, it reaches the periplasm by a holin-independent mechanism.

The activity of Lyz_{103} is regulated by a disulfide "cage." Lyz_{103}, like T4 E but unlike Lyz_{P1}, has an Asp residue as the middle component of its catalytic triad and thus is not regulated by covalent blocking of an active-site Cys (Fig. 1A). Nonetheless, the N-terminal catalytic domain of Lyz_{103} contains three Cys residues (Cys_{12}, Cys_{42}, Cys_{45}), including one in the SAR domain, suggesting that it might exist in two isomeric forms differing in the arrangement of intramolecular disulfide bonds, as documented for Lyz_{P1}. To test this possibility, the C12S mutant of Lyz_{103} was tested for function. This mutant

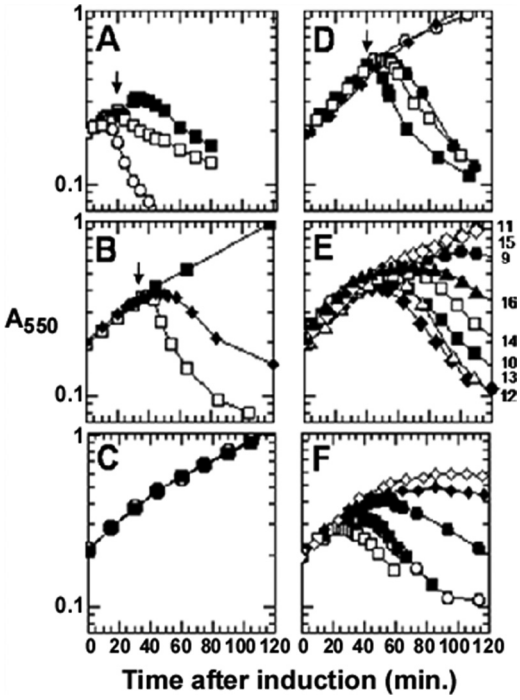

FIG. 2. In each experiment, cultures of XL1-Blue containing Lyz_{P1} or Lyz_{103} in pJF118EH were induced at time zero. The optical density of the culture was followed as a function of time in minutes. (A) Expression of Lyz_{103} lyses the cell independently of a holin. ○, Lyz_{P1}; ■, Lyz_{103}; □, Lyz_{103} plus 10 mM DNP 20 min (arrow) after induction. (B) Lysis by Lyz_{103} is dependent on the SAR domain Cys. ■, Lyz_{103}(C12S); □, Lyz_{103}(C12S) plus 1 mM DTT at 36 min (arrow) after induction; ◆, Lyz_{103}(C12,42,45S). (C) Lyz_{P1} and Lyz_{103} can be locked into the membrane by Leu titration into the SAR domain. ○, Lyz_{103}(G9,10L); ■, Lyz_{P1}(G8,9,10L). (D) Lyz_{P1} and Lyz_{103} can be interconverted. $Lyz_{P1\rightarrow 103}$ was achieved by two amino acid mutations: A41C and C51D (●). $Lyz_{103\rightarrow P1}$ was achieved by two amino acid mutations: C42S and D52C (□). ○, $Lyz_{P1\rightarrow 103}$(C13S); ■, $Lyz_{P1\rightarrow 103}$(C13S) plus 1 mM DTT at 45 min (arrow); ◆, $Lyz_{103\rightarrow P1}$(C12S). (E) There is optimal positioning of the SAR domain Cys. Cys substitutions are labeled adjacent to their respective curves. ●, $Lyz_{P1\rightarrow 103}$(G9C); ■, $Lyz_{P1\rightarrow 103}$(G10C); ○, $Lyz_{P1\rightarrow 103}$(A11C); ◆, $Lyz_{P1\rightarrow 103}$(I12C); △, $Lyz_{P1\rightarrow 103}$; □, $Lyz_{P1\rightarrow 103}$(A14C); ◇, $Lyz_{P1\rightarrow 103}$(I15C); ▲, $Lyz_{P1\rightarrow 103}$(A16C). (F) The placement of the caging disulfide is stringent. ●, Lyz_{P1}(I38C, C51D); ○, Lyz_{P1}(G39C, C51D); ■, Lyz_{P1}(N40C, C51D); □, Lyz_{P1}(C13S, I38C, C51D); ◆, Lyz_{P1}(C13S, G39C, C51D); ◇, Lyz_{P1}(C13S, N40C, C51D).

was found to be lytically inactive (Fig. 2B), although it was released from the inner membrane as efficiently as the wild-type protein (Fig. 3B). Moreover, the addition of the reducing agent, dithiothreitol, to cells expressing the C12S mutant resulted in lysis (Fig. 2B). Finally, the triple mutant, Lyz_{103}(C12,42,45S), was found to be lytically active (Fig. 2B). The behavior of these two mutants is consistent with the model that nascent Lyz_{103} is inactive because of an inhibitory Cys_{42}-Cys_{45} disulfide that is disrupted by Cys_{12} after the release of the SAR domain from the membrane. Since the inhibitory disulfide predicted to exist in nascent Lyz_{103} involves cysteines that flank an essential catalytic residue (Fig. 1A), we refer to it as a "caging" disulfide to distinguish it from the inactivating disulfide present in Lyz_{P1}. It is of interest to note that a similar inactive, disulfide-caged form of T4 gp*e* was constructed 21

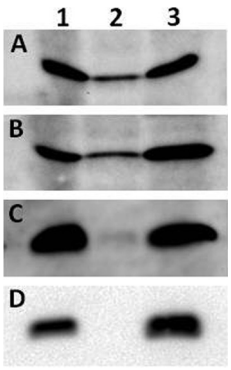

FIG. 3. The endolysins of bacteriophages P1 and ERA103 are SAR endolysins. For all panels, the total protein is represented by lane 1, the soluble protein fraction is represented by lane 2, and the membrane fraction is represented by lane 3. (A) Lyz_{103} exists in the soluble and membrane fractions of the cell. (B) Lyz_{103}(C12S) displays a nonlytic phenotype but is released from the cytoplasmic membrane as efficiently as the wild-type protein. (C) Lyz_{P1} can be confined to the inner membrane by replacing three glycines (residues 8 to 10) with leucine residues. (D) Lyz_{103} can be confined to the inner membrane by replacing two glycines (residues 9 and 10) with leucine residues.

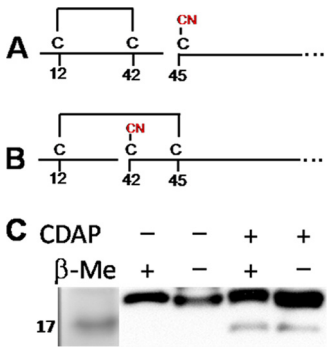

FIG. 4. Analysis of the cage-relieving disulfide. Purified Lyz_{103}(D52N) cHis was subjected to CDAP cyanylation and alkaline cleavage. Proteins were resolved by SDS-PAGE with and without a reducing agent, as indicated. (A) A cage-relieving disulfide between Cys_{12} and Cys_{42} will allow Cys_{45} to be modified by CDAP. Cleavage of this protein results in a C-terminal cleavage fragment that is resolvable without the addition of a reducing agent (β-Me). (B) A cage-relieving disulfide between Cys_{12} and Cys_{45} results in a cleavage product that is resolved only upon the addition of β-Me. (C) Treatment of Lyz_{103}(D52N) with 1,000-fold molar excess of CDAP reagent resulted in a resolvable C-terminal cleavage product (16 kDa), indicating the formation of a Cys_{12}-Cys_{42} disulfide.

years ago (9). In this form of T4 gp*e*, the active-site residues are unaltered but an engineered disulfide occludes the active site. As shown here with Lyz_{103} and earlier with Lyz_{P1}, the disulfide-caged form of T4 gp*e* could be activated by reducing agents.

Disulfide bond isomerization. The results presented above indicate that the Cys_{42}-Cys_{45} disulfide cages the catalytic Glu_{43} in inactive Lyz_{103} and that the Cys_{12} thiol from the SAR domain is required for activation, but the results do not reveal whether one of the two Cys residues flanking Glu_{43} participates in a disulfide exchange with Cys_{12} and, if so, which one (Fig. 1A). To address this question, we used the sulfhydryl cyanylation reagent 1-cyano-4-dimethylaminopyridinium tetrafluoroborate (CDAP). Treatment of a CDAP-cyanylated protein with a strong base cleaves the protein on the N-terminal side of the cyanylated Cys, leaving an N-terminal 2-iminothiazolidine-4-carboxylyl (itz) modification on the C-terminal product (10, 18). If activated Lyz_{103} has a disulfide between Cys_{12} and Cys_{42}, Cys_{45} will be open for CDAP modification and subsequent cleavage would create two polypeptide fragments which could be resolved from uncleaved protein without the presence of a reducing agent (Fig. 4A). In contrast, a linkage between Cys_{12} and Cys_{45} will leave Cys_{42} open for modification. In this case, cleavage with a strong base would result in polypeptide fragments that were still covalently linked and which would require treatment with a reducing agent to be resolved from uncleaved material (Fig. 4B). When purified Lyz_{103} was subjected to CDAP treatment and alkaline cleavage and analyzed by Western blotting with anti-oligo-histidine tag antibodies, a polypeptide product of an appropriate size (16 kDa) could be resolved from uncleaved protein (20 kDa) by SDS-PAGE without a reducing agent (Fig. 4C). The yield of cleavage product was low, approximately 10 to 15% of total protein. However, treatment of the CDAP-modified product with PEG-OPSS revealed that >60% of the protein was cyanylated by CDAP and therefore unPEGylated (data not shown). This indicates that the cleavage reaction, rather than sulfhydryl accessibility, was limiting, presumably due to the high incidence of the competing β-elimination reaction, as noted elsewhere (18). Taken together, these results indicate that the Lyz_{103}-activating linkage resulting from the disulfide bond isomerization after SAR extraction is between Cys_{12} and Cys_{42} rather than between Cys_{12} and Cys_{45}, as predicted from the Lyz_{P1} and Lyz_{103} sequence alignments (Fig. 1A). Thus, the position of the disulfide bond exchange is not conserved.

The Lyz_{P1} and Lyz_{103} regulatory schemes are interconvertible. Comparing the crystal structures of the active and an inactive form of Lyz_{P1} demonstrates that much of the N terminus of the protein is capable of adopting markedly different conformations depending upon the placement of a single intramolecular disulfide (19). To explore the structural malleability of the N-terminal catalytic domain of Lyz_{P1} (Glu_{42}, Cys_{51}, and Thr_{57}), we attempted to convert Lyz_{P1}, in which the inactivating disulfide covalently blocks a catalytic Cys, into a Lyz_{103}-type endolysin, with a caging disulfide sequestering a catalytic Glu, by introducing the A41C and C51D mutations (Fig. 1B, Table 1). This mutant, $Lyz_{P1\rightarrow103}$, was found to be lytically active, although lysis was delayed and more gradual compared with that of the wild-type enzyme (Fig. 2D). As seen with Lyz_{P1}, removal of the SAR domain Cys in $Lyz_{P1\rightarrow103}$(C13S) rendered the enzyme dependent upon the addition of an exogenous reductant (Fig. 2D). Moreover, introducing the C42S and D52C mutations into Lyz_{103} (Fig. 1B) converted the enzyme into a Lyz_{P1}-type endolysin that still required the presence of the Cys residue in its SAR domain for lytic function (Fig. 2D). Thus, with regard to the nature of the inhibitory disulfide and the use of a catalytic Cys or Asp, Lyz_{P1} and Lyz_{103} are fully interconvertible. Since we had polyclonal antibodies at hand for Lyz_{P1} which were much more efficient than the antibodies against the oligo-histidine tag for Lyz_{103}, the $Lyz_{P1\rightarrow103}$ construct was selected for further analysis.

Optimal positioning of the SAR Cys residue. Since we had previously demonstrated that the *in vivo* activity of Lyz_{P1} de-

TABLE 1. Catalytic triads, cysteines participating in enzyme regulation, mutations required for the $Lyz_{P1\rightarrow103}$ and $Lyz_{103\rightarrow P1}$ conversions, and approximate lysis times of Lyz_{P1}, Lyz_{103}, $Lyz_{P1\rightarrow103}$, and $Lyz_{103\rightarrow P1}$[a]

Lysozyme	Catalytic triad	Regulating cysteines	Conversion mutations	Lysis time (min)
Lyz_{P1}	E42, C51, T57	C13 (SAR), C44, C51 (catalytic)	NA	15
Lyz_{103}	E43, D52, T58	C12 (SAR), C42, C44	NA	35
$Lyz_{P1\rightarrow103}$	E42, D51, T57	C13 (SAR), C41, C44	A41C, C51D	50
$Lyz_{103\rightarrow P1}$	E43, C52, T58	C12 (SAR), C44, C52 (catalytic)	C42S, D52C	45

[a] Cysteines located in the SAR domain and catalytic cysteines are indicated. NA, not applicable.

pended upon the placement of the Cys_{13} residue in its SAR domain (19), we reasoned that the poor lytic profile obtained with the $Lyz_{P1\rightarrow103}$ protein might be due to the suboptimal positioning of this critical residue. To test this notion, constructs were generated in which the Cys_{13} residue in the SAR domain was moved to eight new positions, four in each direction, from the parental site in the context of $Lyz_{P1\rightarrow103}$. The results validated the hypothesis, in that earlier and sharper lysis profiles were obtained with a Cys occupying positions 12, 10, 14, and 16, in order of apparent lytic activity (Fig. 2E). This pattern is different from that observed using the equivalent substitutions in Lyz_{P1}, where the Cys_{13} form is the most active and moving the thiol to position 12 eliminated the ability to activate (19). These differences could be due to a combination of factors, since the activation of Lyz_{P1} involves major structural changes within the N-terminal catalytic domain and all of the mutations necessary to convert Lyz_{P1} into $Lyz_{P1\rightarrow103}$ and its derivatives occurred within this domain.

Strict positional requirement for the inhibitory disulfide cage. We next determined the effect of moving the position of the first Cys (Cys_{41}) of the inhibitory disulfide cage in $Lyz_{P1\rightarrow103}$ toward the N terminus of the protein (Fig. 1B). All three variants (N40C, G39C, and I38C) tested were lytic (Fig. 2F). Surprisingly, the lethality of these proteins was not completely dependent upon the presence of a Cys in the SAR domain, as lysis still occurs, although much later and more gradually (Fig. 2F). The simplest explanation for this finding is that disulfides between Cys_{38}, Cys_{39}, or Cys_{40} and Cys_{44} do not effectively cage the active-site glutamate. We directly assessed the status of the cysteines in $Lyz_{P1\rightarrow103}$, $Lyz_{P1\rightarrow103}$(C13S), and Lyz_{P1}(C13S, I38C, C51D), the most lytically active cage mutant, by testing their susceptibility to modification by PEG-OPSS. PEG-OPSS has a PEG 5000 moiety affixed to an orthopyridyl disulfide. When reacted with a free sulfhydryl, PEG-OPSS will covalently bind and will shift the apparent molecular weight of the protein (8). As expected, the active endolysin, $Lyz_{P1\rightarrow103}$, was found to have a single free cysteine (Cys_{13}), while the inactive enzyme, $Lyz_{P1\rightarrow103}$(C13S), had none (Fig. 5). The lytically active Lyz_{P1}(C13S, I38C, C51D) protein was not modified with PEG-OPSS, indicating that all six of its cysteine residues were present in disulfide linkages. Thus, while the Cys_{38}-Cys_{44} disulfide forms, it is not inhibitory.

Conclusion. Two modes of SAR endolysin negative regulation have previously been experimentally established. The first is that of an inactivating disulfide involving a catalytic Cys, as is present in Lyz_{P1} (19); the presence of the disulfide not only precludes participation of the catalytic Cys but also stabilizes a drastically misfolded N-terminal domain. The second mode was found in R_{21}, in which the inactive protein has more subtle folding defects, but the active site is compromised by the proximity of the membrane to which it is tethered by the embedded SAR domain. The results presented here demonstrate that Lyz_{103} represents a third distinct mode of SAR endolysin regulation: disulfide bond caging of the active site in the inactive form of the enzyme (Fig. 6). Despite these differences in the regulatory mode, however, the two proteins appear to be completely interconvertible by simply repositioning the regulatory Cys residues and adjusting the position of the activating Cys residue in the SAR domain. These findings serve to emphasize both the plasticity of the SAR regulatory system and the importance of regulating the timing of lysis in the infection cycle.

Finally, it should be noted that another instance of disulfide

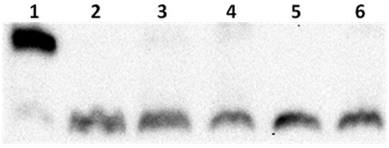

FIG. 5. Assessment of the status of cysteine residues. $Lyz_{P1\rightarrow103}$ is an active endolysin and has a single free sulfhydryl. It is modified by PEG-OPSS (lane 1). $Lyz_{P1\rightarrow103}$(C13S) has no free cysteine residues and is not modified by PEG-OPSS (lane 2). Lyz_{P1}(C13S, I38C, C51D) is an active endolysin despite the presence of the caging disulfide (lane 3). As confirmation of the presence of this disulfide, the protein is not modified by PEG-OPSS, indicating that all of its cysteines are in disulfide bonds. Lanes 1 to 6 contain unPEGylated $Lyz_{P1\rightarrow103}$, Lyz_{P1}(C13S), and Lyz_{P1}(C13S, I38C, C51D), respectively.

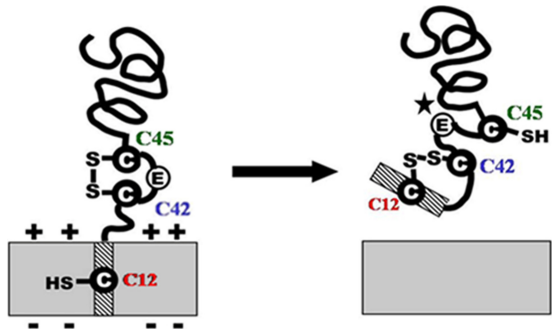

FIG. 6. Model for Lyz_{103} activation. In its inactive form, Lyz_{103} is tethered to the charged cytoplasmic membrane. A caging disulfide exists between Cys_{42} (blue) and Cys_{45} (green) that sequesters the catalytic Glu from the remaining members of the catalytic triad. Upon SAR domain (hatched bar) release from the membrane, the SAR thiol, Cys_{12} (red), attacks the caging disulfide at Cys_{42}, forming a cage-relieving disulfide. The catalytic Glu is released from the cage and can form the catalytic cleft.

bonding affecting the steric blockage of an enzyme active site has been reported in NADP-malate dehydrogenase from chloroplasts (2). In this case, intramolecular steric regulation is achieved when a C-terminal helix, positioned and stabilized by a disulfide bond, occupies the active site and forms hydrogen bonds with catalytic residues. The negative regulation is released when the conserved disulfide is reduced by thioredoxin in response to light stimulation. A key difference is that the Lyz_{103} activation, driven by the release of the SAR domain from the bilayer, is almost certainly irreversible, and thus the stabilities of the inactive and active states are unlikely to be comparable.

ACKNOWLEDGMENTS

Support for this work came from PHS grant GM27099 from the Welch Foundation and also from the Program for Membrane Structure and Function of the Office of the Vice President for Research, Texas A&M University.

The clerical assistance of Daisy Wilbert is gratefully acknowledged.

REFERENCES

1. **Baase, W. A., L. Liu, D. E. Tronrud, and B. W. Matthews.** 2010. Lessons from the lysozyme of phage T4. Protein Sci. **19:**631–641.
2. **Carr, P. D., D. Verger, A. R. Ashton, and D. L. Ollis.** 1999. Chloroplast NADP-malate dehydrogenase: structural basis of light-dependent regulation of activity by thiol oxidation and reduction. Structure **7:**461–475.
3. **Chang, C. Y., K. Nam, and R. Young.** 1995. *S* gene expression and the timing of lysis by bacteriophage λ. J. Bacteriol. **177:**3283–3294.
4. **Furste, J. P., W. Pansegrau, R. Frank, H. Blocker, P. Scholz, M. Bagdasarian, and E. Lanka.** 1986. Molecular cloning of the plasmid RP4 primase region in a multi-host-range tacP expression vector. Gene **48:**119–131.
5. **Gründling, A., U. Bläsi, and R. Young.** 2000. Biochemical and genetic evidence for three transmembrane domains in the class I holin, λ S. J. Biol. Chem. **275:**769–776.
6. **Kim, W. S., and K. Geider.** 2000. Characterization of a viral EPS-depolymerase, a potential tool for control of fire blight. Phytopathology. **90:**1263–1268.
7. **Kim, W. S., H. Salm, and K. Geider.** 2004. Expression of bacteriophage f Ea1h lysozyme in *Escherichia coli* and its activity in growth inhibition of *Erwinia amylovora*. Microbiology **150:**2707–2714.
8. **Lu, J., and C. Deutsch.** 2001. Pegylation: a method for assessing topological accessibilities in Kv1.3. Biochemistry **40:**13288–13301.
9. **Matsumura, M., and B. W. Matthews.** 1989. Control of enzyme activity by an engineered disulfide bond. Science **243:**792–794.
10. **Morreale, G., H. Lanckriet, J. C. Miller, and A. P. Middelberg.** 2003. Continuous processing of fusion protein expressed as an *Escherichia coli* inclusion body. J. Chromatogr. B Analyt. Technol. Biomed. Life Sci. **786:**237–246.
11. **Park, T., D. K. Struck, J. F. Deaton, and R. Young.** 2006. Topological dynamics of holins in programmed bacterial lysis. Proc. Natl. Acad. Sci. U. S. A. **103:**19713–19718.
12. **Smith, D. L., C. Y. Chang, and R. Young.** 1998. The λ holin accumulates beyond the lethal triggering concentration under hyper-expression conditions. Gene Expr. **7:**39–52.
13. **Smith, D. L., D. K. Struck, J. M. Scholtz, and R. Young.** 1998. Purification and biochemical characterization of the lambda holin. J. Bacteriol. **180:**2531–2540.
14. **Smith, D. L., and R. Young.** 1998. Oligohistidine tag mutagenesis of the lambda holin gene. J. Bacteriol. **180:**4199–4211.
15. **Stojkovic, E. A., and L. B. Rothman-Denes.** 2007. Coliphage N4 N-acetylmuramidase defines a new family of murein hydrolases. J. Mol. Biol. **366:**406–419.
16. **Sun, Q., G. F. Kuty, A. Arockiasamy, M. Xu, R. Young, and J. C. Sacchettini.** 2009. Regulation of a muralytic enzyme by dynamic membrane topology. Nat. Struct. Mol. Biol. **16:**1192–1194.
17. **Wang, I. N., D. L. Smith, and R. Young.** 2000. Holins: the protein clocks of bacteriophage infections. Annu. Rev. Microbiol. **54:**799–825.
18. **Wu, J., and J. T. Watson.** 1997. A novel methodology for assignment of disulfide bond pairings in proteins. Protein Sci. **6:**391–398.
19. **Xu, M., A. Arulandu, D. K. Struck, S. Swanson, J. C. Sacchettini, and R. Young.** 2005. Disulfide isomerization after membrane release of its SAR domain activates P1 lysozyme. Science **307:**113–117.
20. **Xu, M., D. K. Struck, J. Deaton, I. N. Wang, and R. Young.** 2004. A signal-arrest-release sequence mediates export and control of the phage P1 endolysin. Proc. Natl. Acad. Sci. U. S. A. **101:**6415–6420.